



OPEN

Stretchable and High-Performance Supercapacitors with Crumpled Graphene Papers

Jianfeng Zang^{1,2,3*}, Changyong Cao^{3*}, Yaying Feng^{3*}, Jie Liu⁴ & Xuanhe Zhao^{3,5,6}

¹School of Optical and Electronic Information, Huazhong University of Science and Technology, Wuhan, Hubei 430074, China, ²Innovation Institute, Huazhong University of Science and Technology, Wuhan, Hubei, 430074, China, ³Department of Mechanical Engineering and Materials Science, Duke University, Durham, NC 27708, USA, ⁴Department of Chemistry, Duke University, Durham, NC 27708, USA, ⁵Soft Active Materials Laboratory, Department of Mechanical Engineering, Massachusetts Institute of Technology, Cambridge, MA 02139, USA, ⁶Department of Civil and Environmental Engineering, Massachusetts Institute of Technology, Cambridge, MA 02139, USA.

Received
12 June 2014Accepted
3 September 2014Published
1 October 2014

Correspondence and requests for materials should be addressed to X.Z. (zhaox@mit.edu)

* These authors contributed equally to this work.

Fabrication of unconventional energy storage devices with high stretchability and performance is challenging, but critical to practical operations of fully power-independent stretchable electronics. While supercapacitors represent a promising candidate for unconventional energy-storage devices, existing stretchable supercapacitors are limited by their low stretchability, complicated fabrication process, and high cost. Here, we report a simple and low-cost method to fabricate extremely stretchable and high-performance electrodes for supercapacitors based on new crumpled-graphene papers. Electrolyte-mediated-graphene paper bonded on a compliant substrate can be crumpled into self-organized patterns by harnessing mechanical instabilities in the graphene paper. As the substrate is stretched, the crumpled patterns unfold, maintaining high reliability of the graphene paper under multiple cycles of large deformation. Supercapacitor electrodes based on the crumpled graphene papers exhibit a unique combination of high stretchability (e.g., linear strain $\sim 300\%$, areal strain $\sim 800\%$), high electrochemical performance (e.g., specific capacitance $\sim 196 \text{ F g}^{-1}$), and high reliability (e.g., over 1000 stretch/relax cycles). An all-solid-state supercapacitor capable of large deformation is further fabricated to demonstrate practical applications of the crumpled-graphene-paper electrodes. Our method and design open a wide range of opportunities for manufacturing future energy-storage devices with desired deformability together with high performance.

Recent advances in materials science and electronics have boomed a nascent field of unconventional stretchable electronics, which can sustain large deformations and conform to surfaces with complicated geometries while maintaining normal functions and reliability^{1–8}. Various stretchable electronic devices have been developed for different applications, such as stretchable circuits⁹, loudspeakers¹⁰, pressure and strain sensors^{2,11}, stretchable transistors¹², epidermal electronics⁷ and implantable medical devices¹³. Since most of the unconventional electronics run on electricity, electrical-energy-storage devices that can be integrated and deformed together with unconventional electronics have become indispensable in achieving fully power-independent and stretchable systems for realistic applications. Recently, novel forms of lithium-ion batteries capable of over 300% deformation have been developed with self-similar serpentine interconnects¹⁴ and origami of thin sheets of the batteries¹⁵, respectively. In comparison with batteries, supercapacitors have the advantages of fast charge/discharge rate and long operating life, and therefore represent a very promising candidate for energy-storage devices in unconventional electronics. Existing stretchable supercapacitors mostly use films or meshes of carbon nanotubes as electrodes^{16–19}. While these carbon nanotube-based supercapacitors can reach stretchability 30% to 100%, synthesis and fabrication of carbon nanotube-based stretchable supercapacitors are complicated and expensive. On the other hand, graphene has an ideal electrochemical capacitance as high as $\sim 550 \text{ F g}^{-1,20,21}$, and graphene-based materials in various forms, including curved graphene²², activated graphene²⁰, vertically oriented graphene²³ and solvated graphene^{24,25}, have been made into supercapacitors with relatively simple fabrication processes and low costs. Despite the promising merits, existing graphene-based supercapacitors only exhibit flexibility and bendability²⁶, but not high stretchability as required in unconventional electronics.



Here, we report a simple and low-cost method to fabricate extremely stretchable and high-performance supercapacitors based on novel crumpled-graphene-paper (CG-paper) electrodes, which demonstrate an unprecedented set of merits including extremely high stretchability (e.g., uniaxial strain $\sim 300\%$, areal strain $\sim 800\%$), high specific capacitance (e.g., $\sim 196 \text{ F g}^{-1}$), and high reliability (e.g., over 1000 stretch/relax cycles). We fabricate graphene paper with high packing density of graphene ($\sim 1.33 \text{ g cm}^{-3}$) and nano-porous structure, which result in its high specific capacitance^{25,27}. The graphene paper is then attached on an elastomer film that has been uniaxially or biaxially stretched to 1.5 \sim 5 times of its original dimensions. Thereafter, as the pre-stretches in the elastomer are relaxed, the lateral dimensions of the adhered graphene paper reduce by the same ratio as those of the elastomer film (Figs. 1a–c). Microscopically, the graphene paper is folded and crumpled into patterns as shown in Figs. 1e and f due to localized mechanical instabilities^{28–30}. When the elastomer film is stretched back, the CG-paper unfolds, enabling extremely high stretchability of the CG-paper electrode. In addition, the high toughness and flexibility of the graphene paper maintains high capacitance and reliability of the electrode under multiple cycles of large deformation.

Crumpling and unfolding graphene paper

Figures 1a–c illustrate the procedure for crumpling graphene papers bonded on elastomer films. A square-shaped elastomer film, VHB acrylic 4910 with thickness of 1 mm (0.104 g mm^{-2} , 3M Inc., US), was biaxially stretched along two orthogonal in-plane directions by strains of $\varepsilon_{pre1} = \Delta L_1/L_1$ and $\varepsilon_{pre2} = \Delta L_2/L_2$, where L_1 and L_2 are the side lengths of the undeformed elastomer, and ΔL_1 and ΔL_2 are the corresponding changes in lengths in the deformed elastomer. Since the elastomer film is highly stretchable, the pre-strains ε_{pre1} and ε_{pre2} are set in a range from 50% to 400%. A graphene paper with thickness in the range of 0.2 \sim 5 μm at the dehydrated state was fabricated following the procedure illustrated in Fig. S1^{25,27}. The as-prepared graphene paper was then bonded onto the pre-stretched elastomer film by a dry-transfer method²⁸ (Fig. S1). Thereafter, the pre-strains

in the elastomer film were relaxed along two directions sequentially (Figs. 1a–c, Fig. S1) to crumple the graphene paper.

When the pre-strain in the elastomer film begins to relax uniaxially along one pre-stretched direction, wrinkles with sinusoidal undulation set in the graphene paper with wavelength^{16,30} $\lambda_{wrinkle} = 2\pi H_f [\mu_f / (3\Lambda\mu_s)]^{1/3}$, where H_f is the thickness of the graphene paper, μ_f and μ_s the shear moduli of the graphene paper and elastomer taken to be neo-Hooke materials, and $\Lambda = [1 + (1 + \varepsilon_{pre1})^2(1 + \varepsilon_{pre2})] / 2(1 + \varepsilon_{pre2})$. The shear moduli of the graphene paper and the elastomer substrate have been measured to be $\mu_f = 19 \text{ MPa}$ and $\mu_s = 20 \text{ kPa}$ (Fig. S2), respectively. Therefore, for a case with $\varepsilon_{pre1} = 250\%$, $\varepsilon_{pre2} = 0\%$ and $H_f = 2 \mu\text{m}$ (Fig. S3), the wavelength of the wrinkle can be evaluated to be 46 μm , which is on the same order as the experimentally measured wavelength ($\sim 78 \mu\text{m}$) of the wrinkles (Fig. S3a).

As the pre-strain in the elastomer further relaxes uniaxially, the amplitude of some wrinkles increase more dramatically than others. Consequently, the initial wrinkles in the graphene paper transit into a pattern of localized ridges, which cease to follow the sinusoidal undulation of wrinkles (Fig. S3)^{28,29}. With further relaxation of the pre-strain, the wavelength of the ridges decreases and the amplitude increases, leading to a pattern of high-aspect-ratio ridges (Fig. S3).

When the pre-strain along the second direction is subsequently relaxed, the pattern formed on the elastomer will be compressed along the ridges, and therefore buckle and collapse. As a result, the biaxial compression of the graphene paper on the highly pre-stretched elastomer film crumples the paper into a pattern as shown on Fig. 1f. While similar crumpling patterns have been observed in nanofilms highly compressed on elastomers^{13,28,29} and vilification of chicken guts³¹, to our knowledge, this is the first demonstration of crumpling graphene papers on substrates.

Furthermore, when the relaxed elastomer film is uniaxially or biaxially stretched, the crumpled-graphene paper will be unfolded, as the amplitude of the ridges decreases and their wavelength increases (Fig. S4). Owing to the relatively high fracture toughness and flexibility of the graphene paper (Fig. S5), the graphene paper can maintain its integrity and electric conductivity over multiple crumpling/unfolding cycles (e.g., over 1000 cycles as shown in

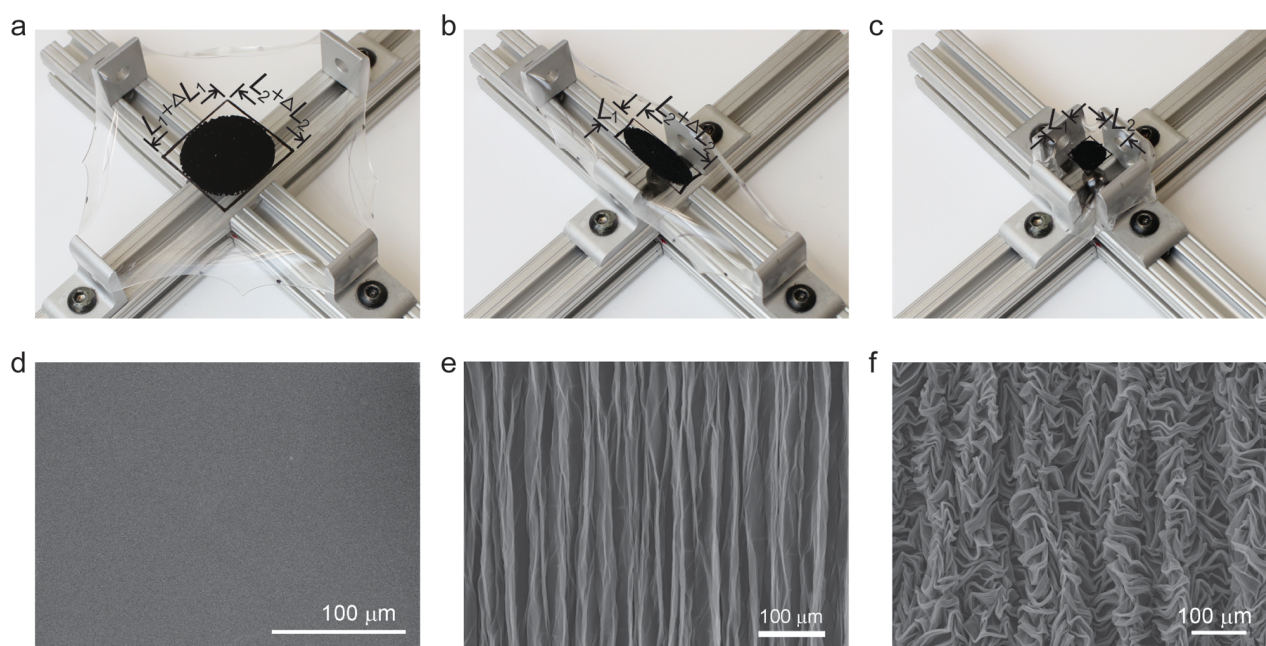


Figure 1 | Fabrication of crumpled-graphene papers. (a–c) Photographs of the simple procedure for crumpling the graphene papers: (a) a flat graphene paper is bonded on a biaxially pre-stretched ($\varepsilon_{pre1} = \varepsilon_{pre2} = 400\%$) elastomer film, which is then (b) uniaxially and (c) biaxially relaxed. (d–f) SEM images of microscopic patterns formed in the graphene paper: (d) the initially flat graphene paper forms (e) parallel ridges as the elastomer film is uniaxially relaxed, and (f) crumpled patterns as the film is biaxially relaxed. The thickness of the graphene paper is $\sim 2 \mu\text{m}$ measured at dehydrated state.



Fig.3b), enabling extremely stretchable and robust electrodes for supercapacitors.

Electrochemical performance of CG-paper electrodes

To demonstrate the stretchability and performance of the CG-papers as supercapacitor electrodes, their cyclic voltammetry (CV) and galvanostatic charge/discharge behaviors were tested in aqueous electrolyte 1.0 M H₂SO₄ solution. The electrodes were fabricated by crumpling graphene papers attached on uniaxially ($\epsilon_{pre1} = 400\%$, $\epsilon_{pre2} = 50\%$, Fig. 2a–c) or biaxially ($\epsilon_{pre1} = \epsilon_{pre2} = 400\%$, Figs. 2d–f) pre-stretched elastomer films.

Figures 2a and d present the CV curves of the CG-paper electrodes in both as-prepared (i.e., crumpled) and highly stretched (i.e., unfolded) states. It can be seen that all the curves exhibit a typical rectangular shape at a scan rate of 50 mV s⁻¹, indicating the behavior of an ideal double-layer electrochemical capacitor. It is noted that weak redox peaks are observed in the CV curves, due to the remaining oxygen-containing groups in the CG-papers. The redox peaks for CG-paper electrodes at stretched states are weaker than those at relaxed states, because the samples were first tested at the relaxed state, during which some oxygen-containing groups were consumed by the electrochemical cycles. In addition, no significant changes are observed in the CV curves of the CG-paper electrodes when they are either uniaxially stretched to strains of 100%, 200% and 300% (Fig. 2a) or biaxially stretched to a strain of 200% × 200%, which is equivalent to 800% areal strain (Fig. 2d). The electrochemical behaviors of the CG-paper electrodes subjected to large deformations were also examined by galvanostatic charge/discharge at different current densities and film thickness, as shown in Figs. 2b, e and Figs. S6–S7. The discharge curves are straight lines, even at current densities as high as 5, 10 and 80 A g⁻¹ (Figs. 2b, e and Fig. S6), which indicates an ideal electrochemical double-layer performance of the

electrodes under large deformation (i.e., uniaxial strain of 300% and biaxial strain of 200% × 200%).

The specific capacitances of the CG-paper electrodes calculated from the discharge slopes at different charge/discharge current densities are given in Figs. 2c and f. We found that the CG-paper electrodes exhibit excellent gravimetric capacitance in the range of 166–196 F g⁻¹ at the operation rate of 1 A g⁻¹. It is also demonstrated that the capacitances of the electrodes are insensitive to large deformation of the electrodes, as long as the applied strains on the CG-paper electrodes are smaller than the pre-strains in the elastomer film during the fabrication process. The high specific capacitance of the CG-paper is attributed to its intrinsic nanoporous structure (Fig. S8) and the pre-trapped electrolyte between individual sheets²⁵. The results are further supported by the electrochemical impedance analysis (Fig. S9) and the scanning electron microscopy (SEM) images of the folded and unfolded CG-paper films, in which no macro-cracks have been observed (Fig. S4). The energy densities of the CG-paper electrodes are calculated to be 28 and 30 Wh kg⁻¹, when subjected to a uniaxial strain of 300% or a biaxial strain of 200% × 200% (Fig. S10). Therefore, the CG-paper electrodes can sustain extremely large deformation either uniaxially or biaxially, while maintaining excellent capacitance.

In order to evaluate the potential of the CG-paper electrodes in practical applications, we further measured the electrochemical performance of the electrodes under multiple cycles of electrochemical and/or mechanical loadings. The electrochemical stability of the stretchable CG-paper electrodes was first evaluated by the galvanostatic charge/discharge cycling as the electrodes were subjected to large deformation. Figure 3a gives the normalized capacitances of the electrodes subjected to a uniaxial strain of 200%, as a function of the numbers of electrochemical charge/discharge cycles at a high current density of 10 A g⁻¹. Except that a very slight decline (about 4% of its initial value) occurs in the first 350 cycles, the capacitance remains unchanged for the rest of the 1000 tested cycles. Similar results were

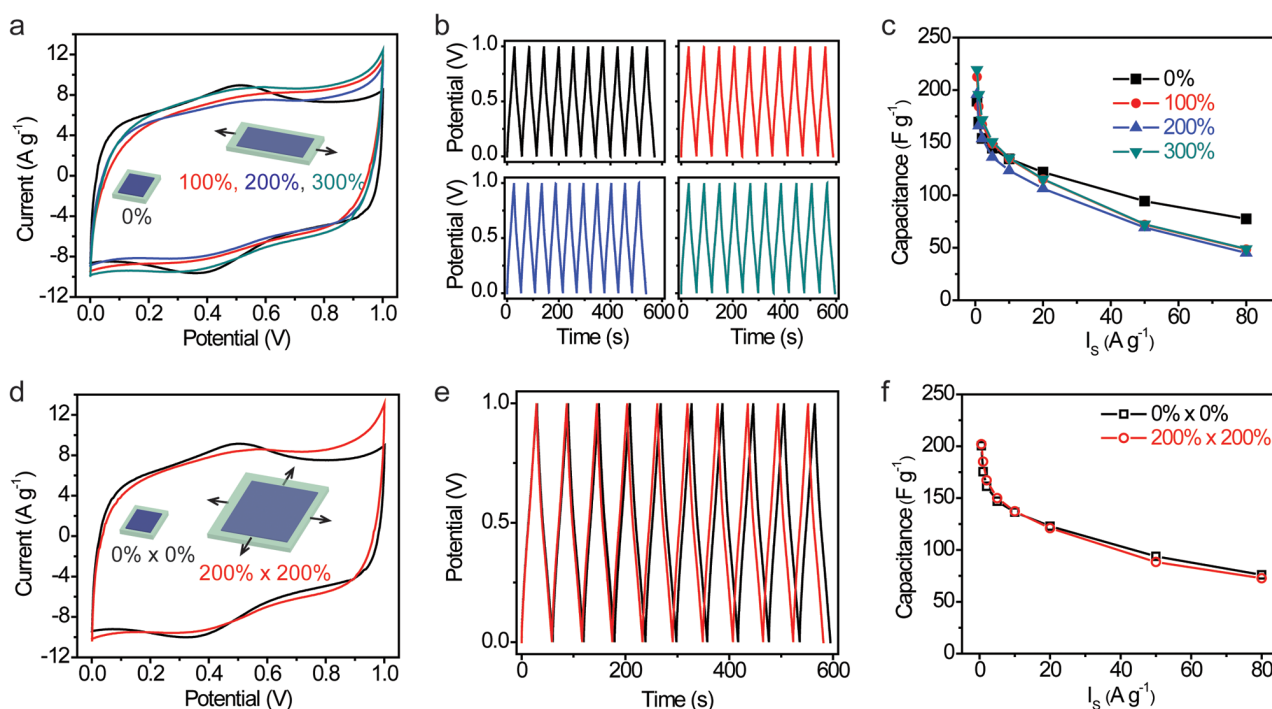


Figure 2 | Electrochemical performance of the crumpled-graphene-paper electrodes under large deformations. Electrochemical characterization of the crumpled-graphene-paper electrodes (a–c) subjected to uniaxial strains of 0%, 100%, 200%, and 300% and (d–f) biaxial strains of 0% × 0% and 200% × 200%. (a, d) Cyclic voltammetry curves at 50 mV s⁻¹, (b, e) galvanostatic charge/discharge curves at 5 A g⁻¹, and (c, f) gravimetric capacitance measured at different charge/discharge current densities ($I_s = 0.5, 1.0, 2.0, 5.0, 10, 20, 50, \text{ and } 80 \text{ A g}^{-1}$). The tests were carried out in 1.0 M H₂SO₄. The thickness of the graphene paper is $\sim 2 \mu\text{m}$ measured at dehydrated state.

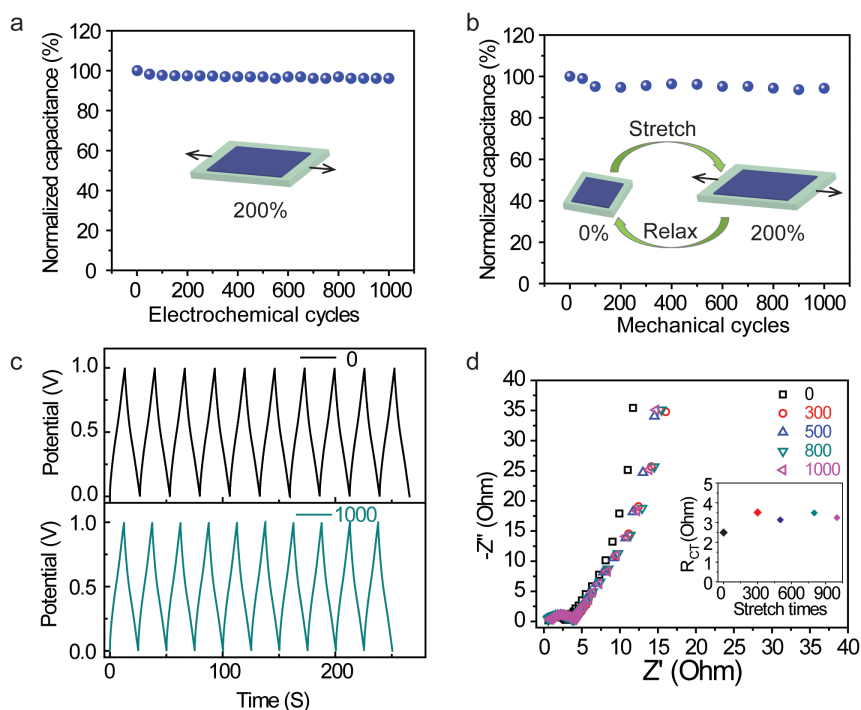


Figure 3 | Electrochemical performance of the stretchable crumpled-graphene-paper electrodes under cyclic electrochemical and mechanical loadings. (a) The normalized capacitance of the crumpled-graphene-paper electrode subjected to a uniaxial strain of 200%, measured by 1000 galvanostatic charge/discharge cycles at 10 A g^{-1} . (b) The normalized capacitance of crumpled-graphene-paper electrode measured by galvanostatic charge/discharge of the electrode in 1000 repeated stretch/relaxation cycles up to uniaxial strain of 200%. (c) Ten cycles of galvanostatic charge/discharge curves at 10 A g^{-1} before and after 1000 stretches to uniaxial strain of 200%. (d) Nyquist plots at the corresponding stretch cycles (0, 300, 500, 800, and 1000). The inset shows the corresponding transfer resistances extracted from (d). The thickness of the graphene paper is $\sim 2 \mu\text{m}$ measured at dehydrated state.

obtained from electrochemical tests on the undeformed electrodes over 5000 charge/discharge cycles (Fig. S11a). In addition, no structural changes were observed in the CG-paper after 5000 cycles (see SEM images in Fig. S11b).

We next carried out electrochemical characterization of CG-paper electrodes under large deformation over multiple cycles. Figure 3b shows the galvanostatic charge/discharge performance of the CG-paper electrode as a function of the number of cycles of uniaxial strain up to 200% applied on the electrode. Remarkably, followed by a slight degradation of $\sim 5\%$ of its initial capacitance (i.e., the capacitance in the undeformed state) in the first 100 cycles, the variation of the capacitance is confined in a very narrow range ($94 \sim 96\%$ of its initial capacitance) for the rest of the 1000 cycles (Fig. 3b, c). The impedance spectra were also recorded to further investigate the influence of cyclic mechanical deformation on electrochemical performance of the CG-paper electrodes. As illustrated in the Nyquist plots in Fig. 3d, the CG-paper electrode displays a similar behavior in the high-frequency semicircle zone before and after experiencing multiple cycles of large deformation. The diameter of the semicircle is related to the charge transfer resistance R_{CT} at the interface of the CG-paper electrode and electrolyte as well as the resistance within the pores of the CG-paper^{24,25,32}. As shown in the inset of Fig. 3d, the extracted R_{CT} remains constantly low ($2.4 \sim 3.5 \text{ ohm}$) during the whole 1000 stretch/relaxation cycles in our experiments. The constantly low R_{CT} indicates that the cyclic large deformation did not significantly increase the transfer resistance of the stretchable CG-paper electrodes or result in a reduction in the performance of the electrodes. Our results have shown an outstanding electrochemical stability of the CG-paper electrodes subjected to multiple cycles of both electromechanical loadings and mechanical stretches, proving the new CG-papers as a promising candidate for highly stretchable and high-performance supercapacitor electrodes.

Stretchable all-solid-state supercapacitors

The development of stretchable ionic conductors, such as hydrogels or polymer electrolytes, offers tremendous opportunity for portable and all-solid-state energy storage devices, thanks to their desirable electrochemical properties, excellent mechanical integrity, and high flexibility and stretchability^{6,32–35}. The highly stretchable and tough hydrogels developed recently can elongate over 20 times of its initial length³⁶, which makes it an excellent platform for fabricating flexible electronics as well as highly stretchable energy-storage devices such as supercapacitors. As demonstrated in Figs. 4a and b, we integrate two stretchable CG-paper electrodes with a stretchable polymer gel, poly(vinyl alcohol) (PVA)- H_3PO_4 , as the electrolyte and separator to fabricate an all-solid-state stretchable supercapacitor. The PVA- H_3PO_4 can be stretched to strains of 300% uniaxially and $100\% \times 100\%$ biaxially without failure (Fig. S12). Figures 4c and d give the CV curves and galvanostatic charge/discharge performance of the supercapacitor under different uniaxial tensile strains. The rectangular shape of the CV curves remains almost unchanged when the integrated device is uniaxially stretched to strains of 50%, 100% and 150%. Remarkably, the large uniaxial strains applied on the device have almost no influence on its electromechanical performance. This is also reflected in the galvanostatic charge/discharge curves given in Fig. 4d, which show nearly symmetric triangular shapes at a current density of 1 A g^{-1} .

We also demonstrated that our device can maintain satisfactory performance when subjected to high biaxial strains. Figure S13 gives the electrochemical performance of the CG-paper-based supercapacitor subjected to biaxial strains. Some degradation of the device's capacitance was observed when the applied biaxial strains reached $50\% \times 50\%$ and $100\% \times 100\%$. The degradation may be explained by the increased contact resistance between the current collectors and CG-paper electrodes, as indicated by the electrochemical impedance spectroscopy (EIS) characterization in Fig. S14.

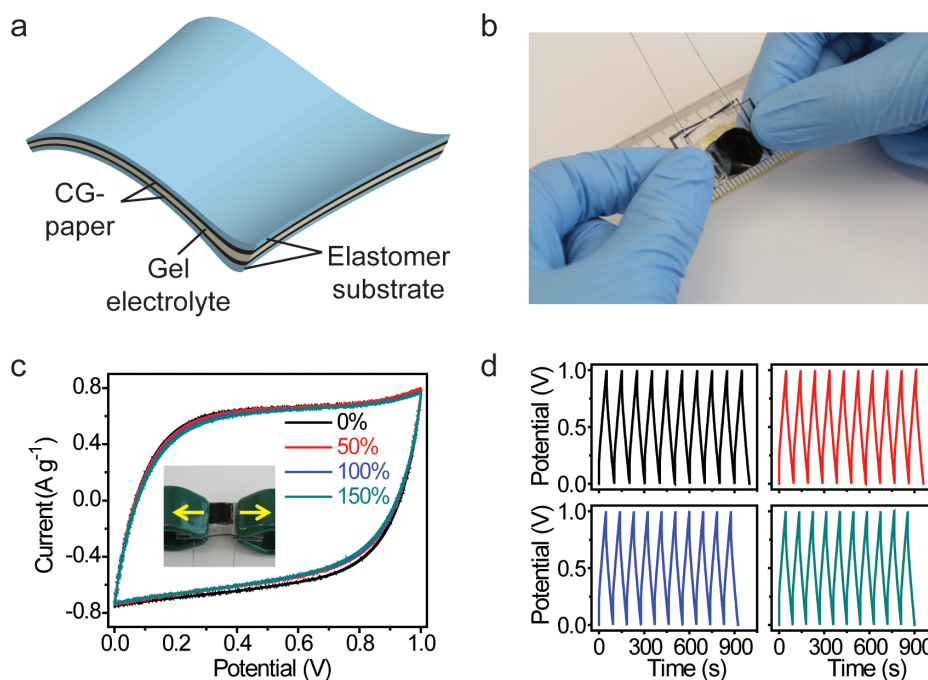


Figure 4 | Design and fabrication of a stretchable all-solid-state supercapacitor with crumpled-graphene-paper as electrodes. (a) A schematic diagram of the supercapacitor using crumpled-graphene-paper electrodes with a polymer electrolyte gel as the electrolyte and separator. (b) Photograph of an assembled device. Large deformation has almost no negative effects on its electrochemical performance, as shown in (c) the CV curves of the supercapacitor collected at a scan rate of 10 mV s^{-1} and (d) galvanostatic charge/discharge curves at a current density of 1 A g^{-1} , under uniaxial strains of 0%, 50%, 100%, and 150%. The thickness of the graphene paper is $\sim 0.8 \text{ }\mu\text{m}$ measured at dehydrated state.

In addition, we presented the self-discharging performance of the supercapacitor in Fig. S15. It can be seen that the supercapacitor shows a low leakage current of less than $13 \text{ }\mu\text{A}$ after 6 h charging (Fig. S15a). After pre-charging to 1 V, the open-circuit voltage of the supercapacitor drops to its 60% in 2.5 h, giving a self-discharging rate of more than 2.5 h (Fig. S15b). It is expected that the performance of the CG-supercapacitor could be further improved by achieving better contacts between electrodes and current collectors and better electrical insulation of the separator between electrodes via innovations in design and integration. The output power can be further enhanced by a rational arrangement of multiple repeat units to form an array structure.

Discussion

Existing flexible or stretchable supercapacitor electrodes are mostly based on nanostructured carbon materials, such as graphene and carbon nanotubes. The graphene-based flexible supercapacitor electrodes have exhibited high specific capacitance (Fig. 5a), for example, 202 F g^{-1} for the laser scribed graphene on polyethylene terephthalate²⁶, 258 F g^{-1} for graphene hydrogels modified with 2-aminoanthraquinone moieties³⁷, 215 F g^{-1} for solvated graphene²⁴, 135 F g^{-1} for chemically modified graphene³⁸, and 170.6 F g^{-1} for liquid-mediated graphene²⁵. These graphene based-supercapacitor electrodes, however, are at most bendable and flexible but not stretchable. Currently, most existing stretchable supercapacitors were fabricated based on buckled macrofilms of either carbon nanotubes or polypyrrole on PDMS^{18,32,39,40}. They can sustain the maximum strain in the range of 30%–120%^{18,32,39,40}, while their specific capacitances are generally in the range of $20\text{--}53 \text{ F g}^{-1}$ (Fig. 5a).

Compared with the existing stretchable electrodes for supercapacitors, our CG-paper electrodes have demonstrated not only outstanding capacitive performance with the specific capacitance in the range of $166\text{--}196 \text{ F g}^{-1}$ at a discharge rate of 1 A g^{-1} , but extremely high stretchability up to 300% linear strain and 800% areal strain (Fig. 5a). At the device level, our CG-paper supercapacitors

have demonstrated not only comparable performance on specific capacitance, in the range of $28\text{--}49 \text{ F g}^{-1}$, but much larger deformability, up to 150% uniaxial strain and $100\% \times 100\%$ biaxial strain (i.e., 300% areal strain) (Fig. 5b and Fig. S13). It should be noted that we used the mass of active materials (i.e., CG-papers) to calculate the specific capacitances and gravimetric energy densities of the electrodes and supercapacitors. While the inactive elastomers will evidently decrease the specific capacitances and energy densities of supercapacitors, very thin elastomer films may be used to minimize this effect. In addition, the elastomers also act as supportive substrates and sealing layers, which are inactive materials commonly used in other supercapacitors too.

The concept of crumpled-graphene paper electrodes conceived here enables us to fabricate supercapacitors with unprecedented mechanical deformability and high capacitive performance using a low-cost and simple fabrication process. The integration of our stretchable supercapacitors with other stretchable devices, such as sensors or actuators, represents a promising direction in developing self-contained stretchable functional units for a wide range of applications (e.g., harnessing instabilities of papers) and materials designs (e.g., nanoporous graphene papers) leads to a general technological route that can empower great potential to fabricate various flexible and stretchable devices, ranging from sensors and actuators to integrated circuits and displays capable of complicated and large deformations. Our method and design may open a new avenue for manufacturing future electronic and energy-storage devices with desired deformability together with high performance.

Methods

Fabrication of graphene paper. Electrolyte-mediated graphene paper was fabricated according to the method reported previously^{25,27}. $100 \text{ mL } 0.5 \text{ mg mL}^{-1}$ highly concentrated graphene oxide (GO) solution (Graphene Supermarket, USA) was mixed with 0.2 mL hydrazine (35 wt% in water) and 0.35 mL ammonia (28 wt% in water) in a glass jar. The jar was heated in an oil bath ($\sim 100^\circ\text{C}$) with vigorous stirring for 3 hr. The reduced graphene oxide solution was then ready for further use.

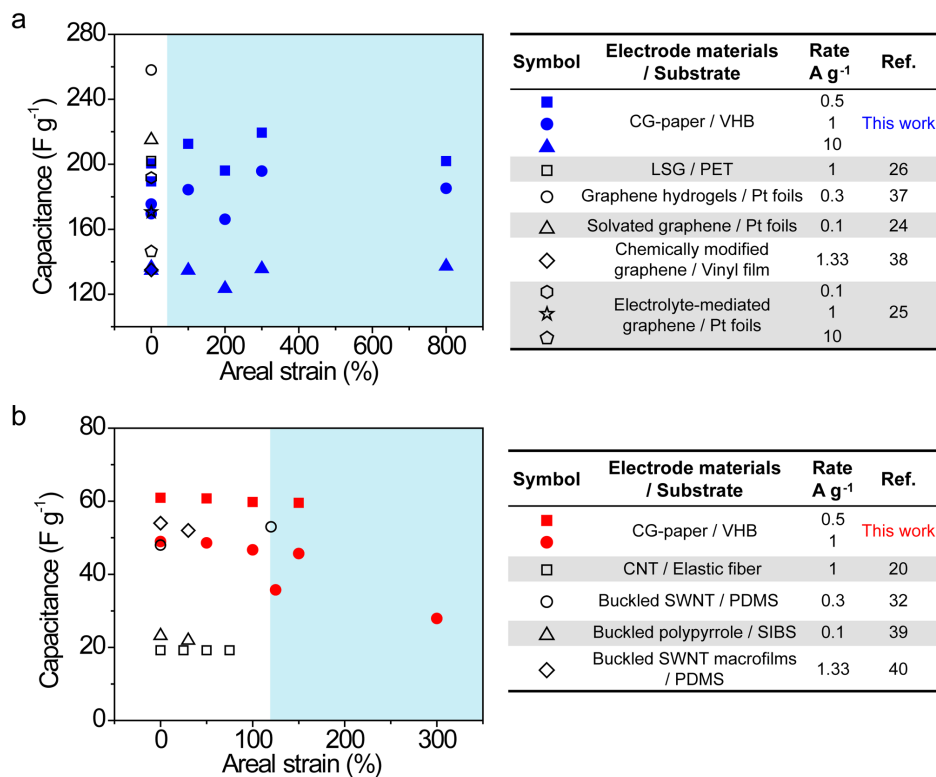


Figure 5 | Comparison of the performances of crumpled-graphene-paper electrodes and supercapacitors with the performances of counter-parts reported in literatures. Capacitances of (a) single electrodes and (b) supercapacitors at different areal strains. The capacitances were measured by galvanostatic charge/discharge at selected current densities, such as 0.5, 1, and 10 A g⁻¹. The shadowed regions in (a) and (b) indicate the unprecedented stretchability achieved by our crumpled-graphene-paper electrodes and supercapacitors. LSG: laser scribed graphene; PET: polyethylene; CNT: carbon nanotubes; SWNT: single-walled carbon nanotubes; SIBS: poly(styrene-block-isobutylene-block-styrene).

Graphene paper in the form of hydrogel was formed by vacuum filtration of the as-prepared reduced graphene oxide solution through a mixed nitrocellulose filter membrane (47 mm in diameter, 0.05 μm pore size, EMD Millipore, USA). The vacuum was immediately disconnected once no reduced graphene oxide solution was left on the surface of filtrated graphene paper. The thickness of each graphene paper fabricated can be controlled by adjusting the volume of the reduced graphene oxide solution, typically 1–30 mL in our experiments. After removing the remaining ammonia and hydrazine by deionized water, the graphene paper was immersed in 5 M H₂SO₄/H₂O miscible solution for 24 hour. The electrolyte of H₂SO₄ was then exchanged with water in the hydrogel of graphene paper and trapped between graphene sheets in graphene paper after vacuum treatment. Then the electrolyte-mediated graphene paper is ready for further use. The as-prepared graphene paper exhibit a porous structure with pore size in the sub-micrometer scale, as shown in Fig. S8. The thickness of the as-obtained graphene paper is in the range of 0.2 ~ 5 μm, which is measured at dehydrated state. The graphene paper with a thickness of 2 μm or 0.8 μm is selected for the electrochemical characterization due to its better rate capability compared with that of thinner graphene paper (e.g. 0.4 μm).²⁷ The graphene paper contains 0.02–0.72 mg cm⁻² graphene. Light microscopy (Nikon ECLIPS LV100) and scanning electron microscopy (FEI XL30 SEM-FEG, USA) were used for morphology characterization of graphene paper at different strains.

Mechanical testing of graphene paper. The mechanical tests, including tensile and trouser tests, were conducted with a micro-strain analyzer (MSA, TA Instruments RSA III). The graphene paper samples were gripped using film tension clamps with a clamp compliance of ~0.2 μm N⁻¹. All tensile tests were conducted in a controlled strain mode with a preload of 0.01 N and a strain ramp of 0.05% min⁻¹ unless otherwise specified. The sample width was measured using a digital caliper. The length between the clamps was automatically measured and recorded by the MSA. The thickness of graphene paper was measured from SEM imaging of the sectioned cross-section of the sample. Bending tests (Fig. S5) were performed under a light microscope. Graphene paper hydrogel film were cut to strips and pressed together using two glass slides. The edges of the graphene paper strip were kept in the same plane. The whole compress process was monitored by a light microscope using 5×, 10× and 20× objectives as needed. The thickness of the graphene paper used in mechanical testing are in hydrate state.

Electrochemical testing of graphene paper. Cyclic voltammetry (CV), galvanostatic charge/discharge and electrochemical impedance analysis were conducted with a Potentiostat (Bio-logic SP300). The graphene paper electrodes were characterized

using a standard three-electrode setup in 1 M H₂SO₄ solution, including a graphene paper electrode as the working electrode, a platinum wire as the counter electrode, and a standard calomel electrode as the reference electrode. All the CV and galvanostatic charge/discharge of both the graphene paper electrodes and the supercapacitors were tested in an operation voltage range from 0 to 1.0 V, and were processed with MATLAB. The electrochemical impedance analysis was conducted at open circuit potential over the frequency range from 200 kHz to 100 mHz. The capacitance and energy density reported here are based on the mass of the active materials (CG-paper) used in the electrodes and the supercapacitors.

Fabrication and electrochemical testing of all-solid-state supercapacitors. The all-solid-state supercapacitor (Figs. 5a and b) was fabricated as follow. Firstly, the poly(vinyl alcohol (PVA) gel electrolyte was prepared. 3 g PVA powder (MW 146000 ~ 186000) was dissolved in 30 mL deionized water. The solution was heated to 90°C under vigorous stirring for about 1 hour until it became clear. 4.5 g H₃PO₄ was then added into the solution and was kept stirring for 10 min and cooled down to room temperature. After degassing in a vacuum chamber overnight, the prepared PVA-H₃PO₄ solution was poured onto the top of the flat graphene paper adhered on a pre-stretched elastomer film (e.g. $\epsilon_{pre1} = \epsilon_{pre2} = 400\%$), and held for 30 min before relaxing the prestrain to allow the solution completely contact the graphene paper. About 0.2–0.5 cm margins of the origami graphene paper surface was left to be uncovered by the solution for electrical contact of the electrode by Pt wire. Then the electrode covered with a liquid layer solution was placed in a fume hood at room temperature for several hours to evaporate the water stored in PVA-H₃PO₄ gel. Finally, the two electrodes were pressed together and heated to 80°C for 10 min to bond the two layers of electrolyte gel into one integrated all-solid-state supercapacitor. The PVA-H₃PO₄ gel between the two electrodes serves as both polymer electrolyte and separator. The all-solid-state stretchable supercapacitors were characterized with a standard two-electrode system.

1. Wagner, S. & Bauer, S. Materials for stretchable electronics. *Mrs Bull.* **37**, 207–217 (2012).
2. Lipomi, D. J. *et al.* Skin-like pressure and strain sensors based on transparent elastic films of carbon nanotubes. *Nat. Nanotechnol.* **6**, 788–792 (2011).
3. Rogers, J. A., Someya, T. & Huang, Y. Materials and Mechanics for Stretchable Electronics. *Science* **327**, 1603–1607 (2010).
4. Kaltenbrunner, M. *et al.* Ultrathin and lightweight organic solar cells with high flexibility. *Nat. Commun.* **3**, 770 (2012).



5. Khang, D.-Y., Jiang, H., Huang, Y. & Rogers, J. A. A Stretchable Form of Single-Crystal Silicon for High-Performance Electronics on Rubber Substrates. *Science* **311**, 208–212 (2006).
6. Keplinger, C. *et al.* Stretchable, transparent, ionic conductors. *Science* **341**, 984–987 (2013).
7. Kim, D.-H. *et al.* Epidermal Electronics. *Science* **333**, 838–843 (2011).
8. Lipomi, D. J., Tee, B. C. K., Vosgueritchian, M. & Bao, Z. Stretchable organic solar cells. *Adv. Mater.* **23**, 1771–1775 (2011).
9. Kim, D.-H. *et al.* Stretchable and foldable silicon integrated circuits. *Science* **320**, 507–511 (2008).
10. Xiao, L. *et al.* Flexible, Stretchable, Transparent Carbon Nanotube Thin Film Loudspeakers. *Nano Lett.* **8**, 4539–4545 (2008).
11. Mannsfeld, S. C. B. *et al.* Highly sensitive flexible pressure sensors with microstructured rubber dielectric layers. *Nat. Mater.* **9**, 859–864 (2010).
12. Lee, S.-K. *et al.* Stretchable graphene transistors with printed dielectrics and gate electrodes. *Nano Lett.* **11**, 4642–4646 (2011).
13. Fu, C. C. *et al.* Tunable Nanowrinkles on Shape Memory Polymer Sheets. *Adv. Mater.* **21**, 4472–4476 (2009).
14. Xu, S. *et al.* Stretchable batteries with self-similar serpentine interconnects and integrated wireless recharging systems. *Nat. Commun.* **4**, 1543 (2013).
15. Song, Z. *et al.* Origami lithium-ion batteries. *Nat. Commun.* **5**, 3140 (2014).
16. Li, X., Gu, T. & Wei, B. Dynamic and Galvanic Stability of Stretchable Supercapacitors. *Nano Lett.* **12**, 6366–6371 (2012).
17. Hu, L. *et al.* Stretchable, Porous, and Conductive Energy Textiles. *Nano Lett.* **10**, 708–714 (2010).
18. Yang, Z., Deng, J., Chen, X., Ren, J. & Peng, H. A Highly Stretchable, Fiber-Shaped Supercapacitor. *Angew. Chem. Int. Ed.* **52**, 13453–13457 (2013).
19. Pushparaj, V. L. *et al.* Flexible energy storage devices based on nanocomposite paper. *Proc. Natl. Acad. Sci. U.S.A.* **104**, 13574–13577 (2007).
20. Zhu, Y. *et al.* Carbon-Based Supercapacitors Produced by Activation of Graphene. *Science* **332**, 1537–1541 (2011).
21. Stankovich, S. *et al.* Graphene-based composite materials. *Nature* **442**, 282–286 (2006).
22. Liu, C., Yu, Z., Neff, D., Zhamu, A. & Jang, B. Z. Graphene-based supercapacitor with an ultrahigh energy density. *Nano Lett.* **10**, 4863–4868 (2010).
23. Miller, J. R., Outlaw, R. A. & Holloway, B. C. Graphene Double-Layer Capacitor with ac Line-Filtering Performance. *Science* **329**, 1637–1639 (2010).
24. Yang, X., Zhu, J., Qiu, L. & Li, D. Bioinspired Effective Prevention of Restacking in Multilayered Graphene Films: Towards the Next Generation of High-Performance Supercapacitors. *Adv. Mater.* **23**, 2833–2838 (2011).
25. Yang, X., Cheng, C., Wang, Y., Qiu, L. & Li, D. Liquid-Mediated Dense Integration of Graphene Materials for Compact Capacitive Energy Storage. *Science* **341**, 534–537 (2013).
26. El-Kady, M. F., Strong, V., Dubin, S. & Kaner, R. B. Laser Scribing of High-Performance and Flexible Graphene-Based Electrochemical Capacitors. *Science* **335**, 1326–1330 (2012).
27. Dikin, D. A. *et al.* Preparation and characterization of graphene oxide paper. *Nature* **448**, 457–460 (2007).
28. Zang, J. *et al.* Multifunctionality and control of the crumpling and unfolding of large-area graphene. *Nat. Mater.* **12**, 321–325 (2013).
29. Cao, C., Chan, H. F., Zang, J., Leong, K. W. & Zhao, X. Harnessing Localized Ridges for High-Aspect-Ratio Hierarchical Patterns with Dynamic Tunability and Multifunctionality. *Adv. Mater.* **26**, 1763–1770 (2014).
30. Zang, J., Zhao, X., Cao, Y. & Hutchinson, J. W. Localized ridge wrinkling of stiff films on compliant substrates. *J. Mech. Phys. Solids* **60**, 1265–1279 (2012).
31. Shyer, A. E. *et al.* Villification: How the gut gets its villi. *Science* **342**, 212–218 (2013).
32. Niu, Z. *et al.* Highly Stretchable, Integrated Supercapacitors Based on Single-Walled Carbon Nanotube Films with Continuous Reticulate Architecture. *Adv. Mater.* **25**, 1058–1064 (2013).
33. Pech, D. *et al.* Ultrahigh-power micrometre-sized supercapacitors based on onion-like carbon. *Nat. Nanotechnol.* **5**, 651–654 (2010).
34. Shi, Y. *et al.* Nanostructured conductive polypyrrole hydrogels as high-performance, flexible supercapacitor electrodes. *J. Mater. Chem. A* **2**, 6086–6091 (2014).
35. Bao, L., Zang, J. & Li, X. Flexible Zn₂SnO₄/MnO₂ Core/Shell Nanocable-Carbon Microfiber Hybrid Composites for High-Performance Supercapacitor Electrodes. *Nano Lett.* **11**, 1215–1220 (2011).
36. Sun, J.-Y. *et al.* Highly stretchable and tough hydrogels. *Nature* **489**, 133–136 (2012).
37. Wu, Q., Sun, Y., Bai, H. & Shi, G. High-performance supercapacitor electrodes based on graphene hydrogels modified with 2-aminoanthraquinone moieties. *Phys. Chem. Chem. Phys.* **13**, 11193–11198 (2011).
38. Stoller, M. D., Park, S., Zhu, Y., An, J. & Ruoff, R. S. Graphene-based ultracapacitors. *Nano Lett.* **8**, 3498–3502 (2008).
39. Zhao, C., Wang, C., Yue, Z., Shu, K. & Wallace, G. G. Intrinsically Stretchable Supercapacitors Composed of Polypyrrole Electrodes and Highly Stretchable Gel Electrolyte. *ACS Appl. Mater. Interfaces* **5**, 9008–9014 (2013).
40. Yu, C., Masarapu, C., Rong, J., Wei, B. & Jiang, H. Stretchable Supercapacitors Based on Buckled Single-Walled Carbon-Nanotube Macrofilms. *Adv. Mater.* **21**, 4793–4797 (2009).

Acknowledgments

The work was supported by ONR (N00014-14-1-0619), NSF (CMMI-1253495, DMR-1121107, EECs-1344745), and the National 1000 Talents Program of China tenable in Huazhong University of Science and Technology (HUST), China. The authors thank Gyeong Hee Lee and Hongbo Zhang for helpful discussion.

Author contributions

X.Z., J.Z. designed the research; J.Z., C.C. and Y.F. performed the experiments; J.Z., C.C. and X.Z. analyzed the data and wrote the paper. J.Z., C.C., Y.F., J.L. and X.Z. discussed and commented on the paper.

Additional information

Supplementary information accompanies this paper at <http://www.nature.com/scientificreports>

Competing financial interests: The authors declare no competing financial interests.

How to cite this article: Zang, J., Cao, C., Feng, Y., Liu, J. & Zhao, X. Stretchable and High-Performance Supercapacitors with Crumpled Graphene Papers. *Sci. Rep.* **4**, 6492; DOI:10.1038/srep06492 (2014).



This work is licensed under a Creative Commons Attribution-NonCommercial-ShareAlike 4.0 International License. The images or other third party material in this article are included in the article's Creative Commons license, unless indicated otherwise in the credit line; if the material is not included under the Creative Commons license, users will need to obtain permission from the license holder in order to reproduce the material. To view a copy of this license, visit <http://creativecommons.org/licenses/by-nc-sa/4.0/>